

RESPONSE OF A SHORELINE SAND WAVE TO BEACH NOURISHMENT

Kathelijne M. Wijnberg¹, Stefan G.J. Aarninkhof² and Ruud Spanhoff³

On Egmond beach, The Netherlands, the trough of a shoreline sand wave was filled by a beach nourishment. Monthly monitoring over a 4 year period revealed that the shoreline sand wave recovered in about half a year, exhibiting an amplitude that exceeded the pre-nourishment one. The more rapid response of the lower elevation contours relative to the higher elevated ones resulted temporarily in beach steepening in the trough area and flattening in the crest area. A first comparison to similar time-scale (months) variations in wave conditions revealed neither evidence that the shoreline sand wave amplitude would tend to flatten during high energetic conditions nor that it would tend to grow under high-angle incident waves. The role of the slowly evolving nearshore morphology and its effects on the nearshore flow field at the monthly time-scale need further study.

INTRODUCTION

Shoreline sand waves are common features along sandy beaches. This type of sea bed feature may be best described as consisting of quasi-periodic features that emerge along the interface of the land and the sea on sandy coastlines (Fig.1). Typically, the alongshore length (or crest spacing) of these features is of order km, which lead others to refer to these features as 'giant cusps' or 'mega cusps'. Their spatio-temporal evolution (alongshore migration, as well as amplitude evolution) adds considerable variability to any long-term trends in the evolution of the average shoreline position. This variability can lead to temporary problems regarding beach recreation as well as coastal safety (i.e. locally increased probability of critical amounts of dune erosion leading to damage to sea-side property or, in worst-case scenarios, to flooding of the hinterland). Local protection measures may be needed to solve these problems.

Today, intervention in the coastal system often involves soft remedial measures like beach nourishment. A clear advantage over hard remedial measures is that it adds sediment to the system where obviously a local shortage exists. On the aggregated scale of annual sediment budgets this may be perceived as a good solution. However, locally this may not necessarily be the case, because the added sediment will generally be redistributed non-uniformly by natural processes. Since pattern formation is omnipresent in natural systems, the local addition of sediment to the beach may potentially enhance the pattern

¹ Water Engineering and Management, University of Twente, P.O. Box 217, 7500 AE Enschede, The Netherlands

² WL|Delft Hydraulics, P.O. Box 177, 2600 MH Delft, The Netherlands (now at Royal Boskalis Westminster, P.O. Box 43, 3350 AA Papendrecht, The Netherlands)

³ Rijkswaterstaat RIKZ, P.O. Box 20907, 2500 EX The Hague, The Netherlands

formation mechanisms. In the worst case, this redistribution process locally leads to enhanced problems. A combined shoreface-beach nourishment applied to Egmond beach in 1999 serves as an example of such a case, where in July 2000 an additional beach nourishment had to be applied in the ‘trough’ of an evolving shoreline sand wave.



Figure 1. Shoreline sand waves near Egmond aan Zee, The Netherlands.

In this paper we will describe the evolving shoreline sand wave over a 4 year period including the response to the July 2000 beach nourishment. In order to understand the mechanisms that caused the observed shoreline sand wave behavior, the variations in forcing conditions that occurred over the period of study need to be analyzed as well. In this paper we will present a first explorative analysis in that direction. To that end, the viability of two hypotheses will be explored: (1) the amplitude of a shoreline sand wave will be damped during periods of high energetic conditions (classical view of shoreline straightening during storms conditions), (2) the amplitude of a shoreline sand wave will grow during conditions of high-angle incident waves (related to the morphodynamic instability hypothesis recently proposed by Ashton et al. (2001) and extended by Falques and Calvete (2005)). In both cases we assume that the observed evolution of the shoreline sand wave is related to variation in the forcing conditions at matching time-scales (months-seasons) (cf. the primary scale relationship proposed by De Vriend, 1991).

STUDY AREA AND DATA SETS

Study area

Egmond beach is located on the west coast of the Netherlands, facing the southern North Sea. It is fronted by 2 subtidal bars, and the medium to fine sand intertidal beach often exhibits a low-tide terrace / ridge and runnel type

topography. The tide is semi-diurnal with a range of about 1.8 m. The mean annual wave height (H_{rms}) is 0.88 m. Wave heights vary on a seasonal basis, ranging from mean monthly H_{rms} wave heights of about 0.7m from May to August, to about 1.25 m in December and January (Wijnberg, 2002).

Since June 1999, the beach and nearshore in front of Egmond are monitored by a 5-camera Argus video system, mounted on the Egmond light house. Every hour during daylight the cameras collect (amongst others) 10-minute time exposure images, which can be used to map the intertidal beach bathymetry (see section on 'Data set beach morphology')

In April 1999, a beach nourishment was applied along the full stretch of the studied beach. Subsequently, the shoreface was nourished at about 5m depth at the seaward side of the outer bar (Table 1). In July 2000, an additional beach nourishment was applied in the 'trough' of the evolving shoreline sand wave (see Table 1 for nourishment details).

<i>date</i>	<i>type</i>	<i>Alongshore extent</i>	<i>Amount (m³/m)</i>
April 1999	beach	-750m to 750 m	200
June-Sep 1999	shoreface	-1100m to 1100m	400
July 2000	beach	0 to 750 m	250

Beach morphology data set

A dataset of monthly surveys of the intertidal beach bathymetry was generated with the help of the Intertidal Beach Mapper (IBM, Aarninkhof et al., 2003). The IBM model determines the three-dimensional beach surface between the low-tide and high-tide shoreline contours by mapping a series of beach contours from Argus video time exposure imagery, sampled throughout a tidal cycle.

The present study involves a compilation of three data sets: two existing bathymetrical datasets generated by Caljouw (2000) and Nipius (2002) for the periods June 1999 – June 2000 and July 2000 – September 2001, respectively, and a newly generated dataset for the period October 2001 – May 2003. Due to variations in the spatial extent of the three datasets, only the overlapping region could be taken into account. This limitation reduced the intertidal study area to a 1360 m coastal strip centered around the Egmond light house and enclosed by the elevation contours at 0m NAP and +0.9 m NAP. The overall dataset thus obtained consists of 48 monthly intertidal beach bathymetries over the period June 1999 – May 2003.

The method of mapping beach topography by measuring the position of elevation contours (as opposed to measuring the elevation at fixed spatial positions) results in a time-varying location of the mapped area. Therefore, it follows naturally that an analysis of the position of selected elevation contours uses the gathered data most efficiently.

The contour position is measured relative to a local coordinate system, of which the alongshore axis roughly parallels the foredune, and the cross-shore axis is defined positive in offshore direction. The origin is at beach pole RSP 38.00, located approximately in front of the Egmond lighthouse.

The lowest common contour for the three constituent data sets is the 0m NAP contour and the highest is the +0.9m NAP contour, which approximates mean high tide level. Since the 0m contour position was occasionally somewhat affected by interpolation effects (in the early observations of the Caljouw data set) the +0.2m NAP contour was added for analysis.

Wave data set

Offshore wave conditions (root mean square wave height H_{rms} , peak period T_{peak} and angle of incidence θ_0) were measured every three hours with a directional wave buoy at IJmuiden, located approximately 15 km to the south of the monitored site. Missing data were sampled from a similar wave station at Eierland, located approximately 75 km to the north of Egmond. Only five data gaps remained: two 0.5 day gaps, a 4 and a 6 day gap, and a 1 month gap, the latter occurring in 1999 from October 18 to November 17. During the 4 year study period, the mean H_{rms} wave height was 0.85 m, with H_{rms} in exceedance of 3.5 m during 8 distinctive storm events.

The viability of the hypothesis of shoreline straightening during energetic conditions will be explored by analyzing the cross-shore component E_{sn} of the nearshore wave energy flux, formulated as:

$$E_{sn} = \frac{1}{8} \rho g H_{rms}^2 c_g \cos(\theta) \quad (1)$$

In Eq. (1), c_g is the wave group velocity, H_{rms} is the root mean square wave height and θ is the wave angle of incidence with respect to shore normal, all evaluated at the NAP-6m depth contour, which approximates the seaward end of the nearshore bar zone. Offshore wave conditions were translated to the NAP-6m depth contour with the help of a standard parametric wave model (Battjes and Janssen, 1978), accounting for wave refraction, bottom friction and wave breaking. Offshore tidal levels were interpolated from water level data collected at two tidal station located 15 km north and south of Egmond. Missing values were replaced by astronomical predictions.

Exploring the viability of the ‘high-angle wave instability’ mechanism includes separating the waves arriving from the two opposite quadrants of the shore normal direction. Since the shore normal direction points almost straight to the West (viz. 278° with respect to the North), these quadrants are referred to as the ‘NW’ and ‘SW’ quadrant, representing waves arriving from respectively the clockwise and anti-clockwise directions relative to the shore normal direction.

METHODOLOGY

Morphological evolution

Since this study focuses on the evolution of the sand wave, we first remove the alongshore averaged position of the contour (which represents the average onshore and offshore movement of the beach as a whole). Next we analyze the residuals, i.e. the deviations from the average on-offshore movement of the beach, with the EOF-analysis technique (Winant et al., 1975).

The analyzed data matrix $[D]$ consists of N_t observations of contour position ($N_t = 48$), and the cross-shore position of each contour is described at N_y longshore positions ($N_y = 69$), such that:

$$[D] = [X] - [M] \quad (2)$$

where:

$[X]$ = $N_y \times N_t$ raw data matrix of contour positions or beach width.

$[M]$ = $N_y \times N_t$ matrix, containing in each column the mean value of the matching column in $[X]$.

In order to quantitatively compare the amount of variability included in longshore-averaged behavior versus that in spatially coherent behavior, we calculated the variance of all elements in $[M]$ and of all elements in $[D]$. The sum of these two equals the variance of all elements in $[X]$. We refer to the latter as the total amount of variance.

Through a singular value decomposition of $[D]$,

$$[D] = [U] \cdot [S] \cdot [V]' \quad (3)$$

we derive the matrices $[U]$, $[S]$, and $[V]$, where $[U]$ is a $N_y \times N_t$ matrix containing the spatial EOFs and $[V]$ is a $N_t \times N_t$ matrix containing the associated temporal EOFs. $[S]$ is a $N_t \times N_t$ matrix containing the singular values of $[D]$; all off-diagonal values of $[S]$ are zero. The amount of variance that is explained by each EOF mode can be derived from $[S]$, according to:

$$[E] = (N_y - 1)^{-1} \cdot \text{diag}([S] \cdot [S]') \quad (4)$$

where $[E]$ is a vector containing the variance explained by each subsequent EOF mode. The sum of all elements in $[E]$ equals the total amount of variance in $[D]$. For presentation purposes the temporal EOFs will be scaled ($[V]_{\text{scaled}}$) with the standard deviation they represent, such that their magnitudes reflect their contribution to the total signal (see Figure 3c):

$$[V]_{\text{scaled}} = (N_y - 1)^{-0.5} \cdot [V] \cdot [S] \quad (5)$$

Relating morphologic evolution to wave conditions

Since we adopted the assumption of primary scale relationship, the time series of 3-hourly observations of wave conditions are passed through a

Hanning filter with a 90 day window width, prior to comparison to the morphologic evolution. This filtering procedure reveals fluctuations in the wave forcing at a time-scale that is similar to that of the morphologic observations (monthly sampling). Note that the remaining data gaps in the wave time series (see section on data sets) were linearly interpolated prior to applying the filter.

The monthly observations of shoreline position will also contain some ‘contamination’ by short term variability. Therefore, the time series describing the sand wave evolution, as represented by the temporal EOFs, were linearly subsampled to obtain three-hourly observations and passed through the same 90 day Hanning filter.

RESULTS

Beach evolution

Over the studied 4 year period, the alongshore uniform movement of the beach (=on/offshore movement of the complete beach, Fig. 3a) appeared to contain only 23-30% of the total variance (Table 2). Of the remaining 70-77% of variance, the majority (84-86%, or 59-67% of *total* variance) was related to the evolution of a pattern described by EOF1. The remaining variability (which amounted to 11-12% of the *total* variance) could not be attributed to patterns that were statistically significant, that is, the patterns of higher mode EOFs could well be just random mixtures of the true underlying patterns (Fig. 2) (North et al., 1982).

The dominant morphological pattern described by EOF1 appears to represent the shoreline sand wave (Fig. 3b) and its amplitude evolution over time (Fig. 3c). Note that the currently used data set does not cover its full length, which is probably around 2 km, the typical shoreline undulation length scale along this part of the coast for decades (e.g. Stive et al., 2002). The temporal pattern shows an overall increase in amplitude towards a ‘maximum’ in the period January-July 2001, followed by a decrease that may have reached its ‘minimum’ in the beginning of 2003. A clear disturbance of this overall pattern is caused by the July 2000 beach nourishment. The amplitude of the undulation drops to almost zero due to the beach nourishment, because the landward

	0 m contour	+0.2 m contour	+0.9 m contour
Alongshore average ([M])	30.0	26.4	22.6
Residuals ([D])	70.0	73.6	77.4
<i>EOF1 of residuals</i>	58.5 (83.6)	61.7 (83.8)	66.7 (86.1)
<i>EOF2 and higher modes</i>	11.5 (16.4)	11.9 (16.2)	10.7 (13.9)

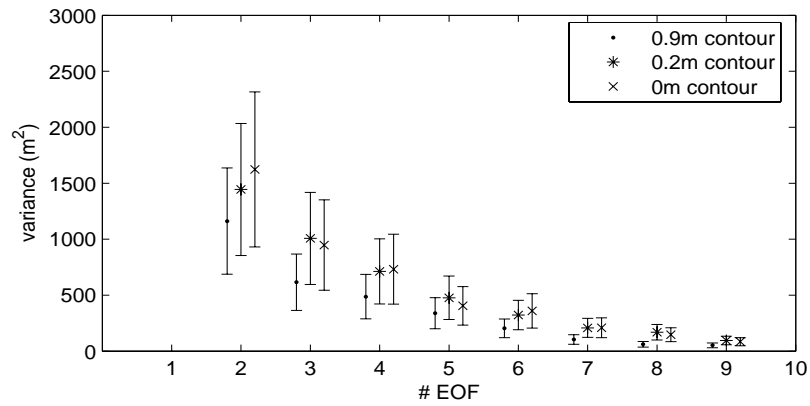


Figure 2. Amount of variance (m^2) attributed to subsequent EOFs, for each of the 3 contour data sets (EOF1 with error bars is out of scale). Error bars indicate 2 times the standard error of the variance estimator (see North et al., 1982).

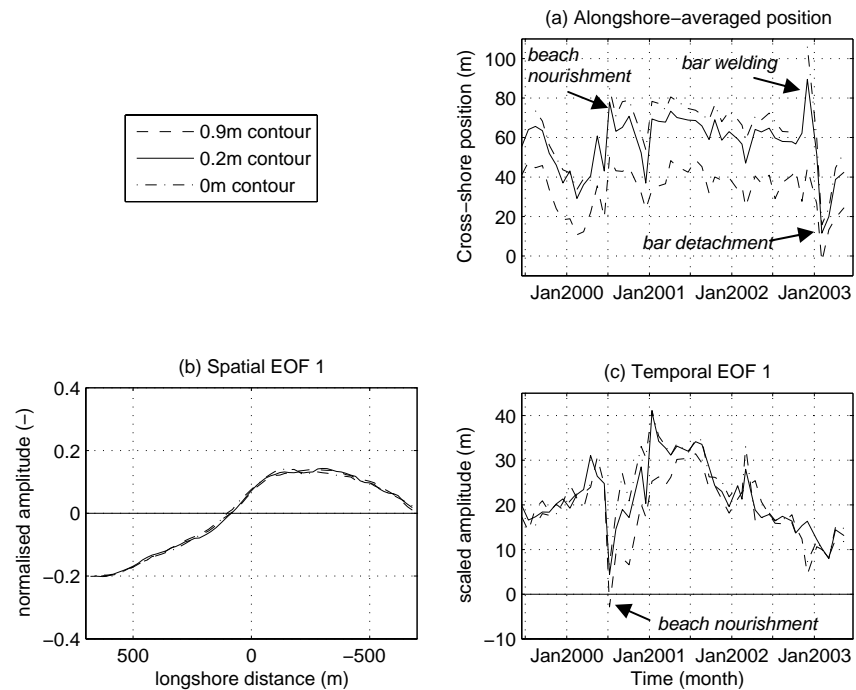


Figure 3. (a) Alongshore-averaged contour position, (b) First spatial EOF, (c) First temporal EOF, scaled with the square root of the amount of variance it explains.

directed part of the undulation has been filled with the nourishment. The nourishment material is incorporated in the natural pattern in a matter of months.

The shapes of spatial EOF1 are almost identical for the 3 studied contours (Fig. 3b), contrary to the patterns of their temporal evolution (Fig. 3c). Interestingly, the +0.9m contour seems to adapt more slowly after the nourishment than the lower elevation contours (0m and +0.2m). Also, for the lower elevated contours (0m and 0.2m contour) the maximum amplitude after nourishment is larger than that prior to nourishment.

The difference in response time implies steepening of the beach in the 'trough' area and widening in the 'crest' area occurring at the same time. This correlation suggests that the sediment from the developing shoreline 'trough' is deposited in the shoreline 'crest' region.

After the nourishment has been completely absorbed in the natural pattern (roughly a year) a consistent difference in amplitude depending on contour elevation is no longer apparent

Correlation with wave conditions

The wave forcing, in terms of cross-shore wave energy flux, is clearly seasonal in nature (Fig. 4a). A matching seasonality in sand wave amplitude evolution, however, is absent (Fig. 4b). The hypothesis of shoreline straightening (i.e. sand wave amplitude decrease) during periods of increased levels of cross-shore wave energy flux is not supported by the data, hence does not seem to represent a dominant mechanism on this beach.

Falques (2006) concluded that the stretch of coast that includes Egmond beach is potentially morphodynamically unstable to wave-driven longshore transport under high-angle incident waves. This would imply that the period of shoreline amplitude growth would go with relatively large angles of wave incidence compared to the period of shoreline amplitude decay. Wave angles of at least 42° are theoretically needed for the growth of shoreline sand waves (e.g. Falques and Calvete, 2005).

The observations show that the magnitude of the angles of incidence is sufficient to cause shoreline instability (Fig. 4c), but the wave angles during periods of shoreline amplitude growth are not very different from those occurring during the period of amplitude decrease (Fig. 4c). This also holds when considering waves from the 'NW'-quadrant separately from those arriving from the 'SW'-quadrant (both defined relative to the shore normal direction).

Falques and Calvete (2005) argued that offshore wave steepness affects the critical angle at which instability can occur, being larger for less steep waves. The variation in wave steepness, which scales with H/T^2 , (Fig. 4d), does not seem to improve support for the mechanism of morphodynamic instability, because the more obliquely incident north-westerly waves tend to be less steep (resulting in larger critical angles) than the less obliquely incident south-westerly waves.

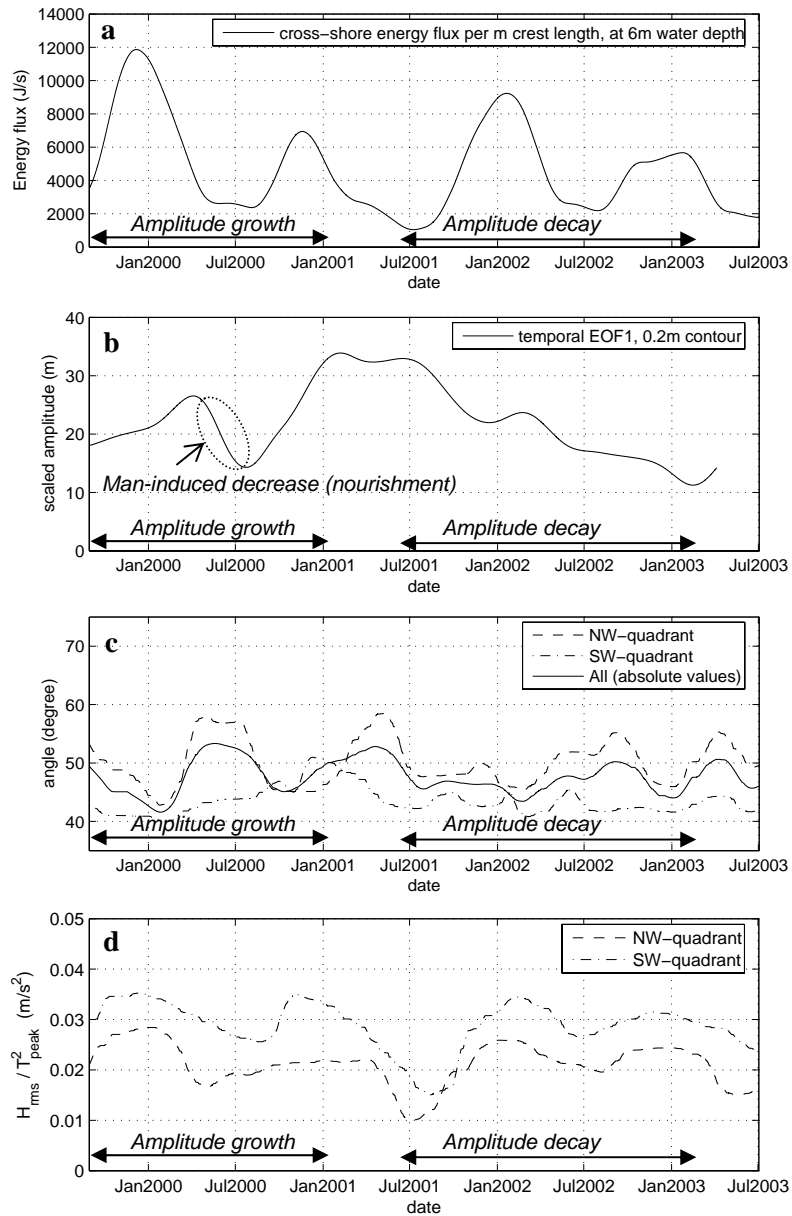


Figure 4. Shoreline sand wave amplitude evolution and seasonal scale variation in wave conditions. (a) cross-shore energy flux (6m depth), (b) Shoreline sand wave amplitude evolution (EOF1, 0.2m contour), (c) absolute angle of incidence relative to shore normal (deep water), (d) wave steepness proxy (deep water). All are passed through a 90-day Hanning filter.

ON THE ROLE OF NEARSHORE MORPHOLOGY

A first comparison of shoreline sand wave amplitude evolution to variation in wave conditions on similar time scales (monthly/seasonal) does not provide support for mechanisms that directly link properties of offshore wave conditions to a preferred response of the shoreline configuration. A possible explanation for the limited reflection of wave forcing seasonality in the evolution of the beach may be found in the non-seasonal evolution of the nearshore bathymetry, which modifies the incoming wave field at an according time-scale.

The nearshore bathymetry in front of the study area is characterized by the presence of a nearshore bar system which exhibits a multi-annual cyclic evolution that seems unrelated to a matching multi-annual cycle in wave forcing (Wijnberg and Kroon, 2002). In addition, a shoreface nourishment was placed right in front of the study area (Table 1). Note that over the studied time-scale no sediment from the shoreface nourishment would have actually reached the beach (Van Duin et al., 2004).

Based on 13 bathymetric surveys obtained between June 1999 and May 2003, covering a 13 to 18 km stretch of coast about 1200m wide (see Fig. 5), a qualitative comparison was made between the beach evolution and the evolution in the nearshore bathymetry. These surveys showed that:

- The study area was in a zone with potential for the occurrence of a ‘bar-switching’ event, because of the alongshore difference in the decay stage of the outer bar (Fig. 5a). Bar switching involves shore-parallel bars becoming discontinuous, with the landward bar on one side of the discontinuity realigning and joining the more seaward bar on the other side (Wijnberg and Wolf, 1994; Shand et al., 2001)
- The location of the shoreface nourishment seems to have ‘attracted’ the occurrence of the bar-switching event in front of the study area (Fig. 5a,b,c)
- During the bar-switching event, the phase relation between bar undulations and beach undulations changes. Prior to the bar-switching (Fig. 5a), the rhythmicity in the bar is in anti-phase with the beach undulation. As the ‘middle’ bar north of the study area attaches to the shallow inner bar south of the study area, the bar rhythmicity is in phase with the beach undulation (Fig. 5c). This situation coincides with the period of largest amplitude in shoreline undulation, as described by EOF1.
- The in-phase relationship ends when the ‘new’ bar straightens out (Fig. 5d, e) (followed later on by formation of rhythmicities on a different scale), which goes with a decrease in shoreline undulation amplitude. Whether this is a coincidental or causal relation requires further research.

The bar-switching event is not a seasonal event, hence its effect on the nearshore flow field extends over several seasons. Apparently, these effects seem to exceed the influence of the clearly seasonal variation in offshore wave conditions.

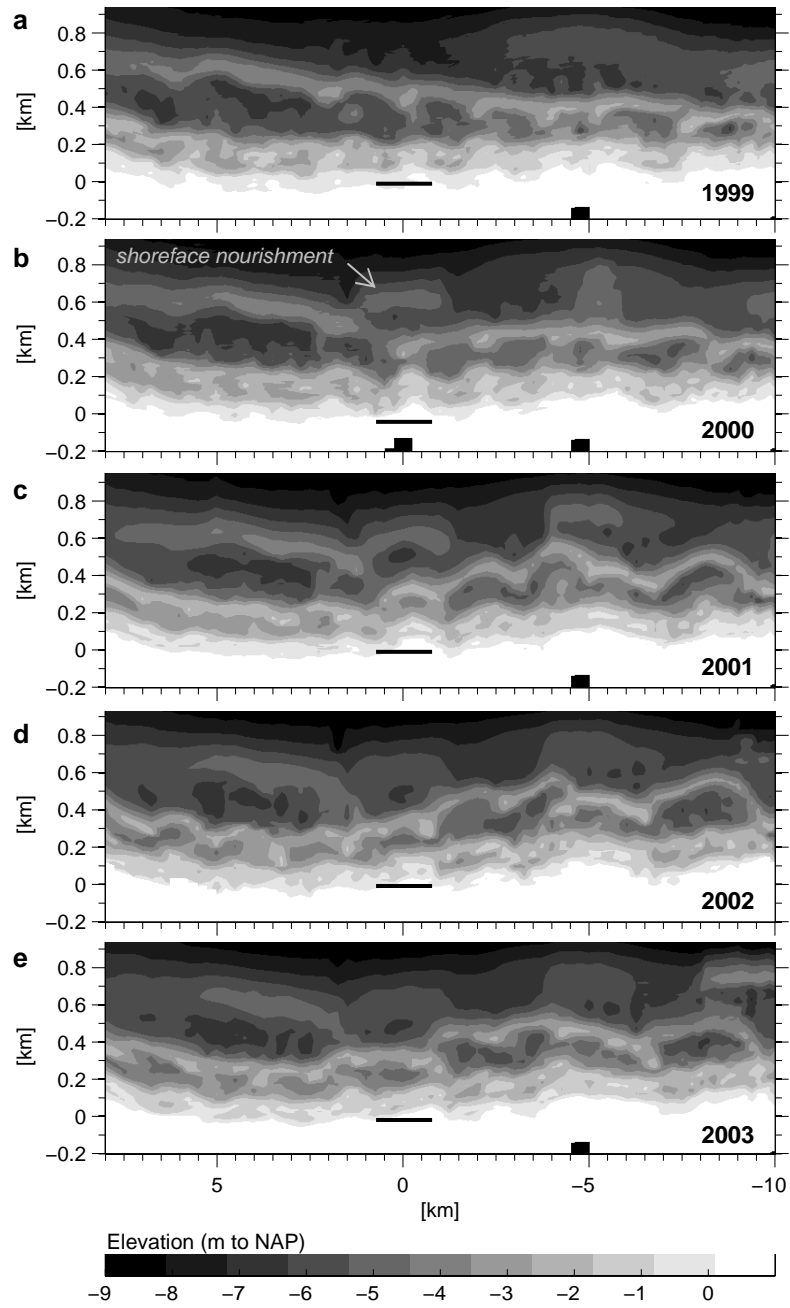


Figure 5. Nearshore bathymetric evolution near the study area, from 1999 (prior to nourishment) to 2003. The horizontal bar indicates the location of the study area.

CONCLUSIONS

The morphological analysis showed that, at the considered scales (1.4 km of beach, 4 year, monthly sampling), evolution of the shoreline sand wave amplitude was the dominant signal on this beach (59%-67% of total variance in shoreline position). Only about a quarter (23%-30%) of the total variance in shoreline position could be attributed to on-offshore movement of the complete beach (i.e. alongshore uniform movement). The remainder of the shoreline variability (about 11% of the total variance) could not be attributed to statistically significant patterns.

The input of sediment by the beach nourishment seems to have favored amplitude growth of the shoreline sand wave beyond its pre-nourishment amplitude. A comparison to the observed variation in wave conditions at comparable time scales (i.e. monthly/seasonal) provides no support for either the mechanism of shoreline straightening under high energetic condition, or for the mechanism of shoreline instability under high-angle incident waves. However, the presented comparison was intended as only a first step in the analysis and further study is needed on the role of the slowly evolving nearshore morphology in modulating the incoming wave field at the monthly time-scale.

ACKNOWLEDGMENTS

At the time of the actual research both Wijnberg and Aarninkhof were employed at WL|Delft Hydraulics and conducted this research in the framework of the EU-funded project Coastview under contract number EVK3-CT-2001-0054. Mark Caljouw, Leann Nipius and Cynthia Reintjes are warmly thanked for collecting the shoreline data from the Argus video imagery. In addition, Rijkswaterstaat is acknowledged for supplying the wave and water level data and bathymetric data.

REFERENCES

- Aarninkhof, S.G.J., I.L. Turner, T.D.T. Dronkers, M. Caljouw, and L. Nipius. 2003. A video-technique for mapping intertidal beach bathymetry. *Coastal Engineering*, 49, 275-289.
- Ashton, A., A.B. Murray, and O. Arnault. 2001. Formation of coastline features by large-scale instabilities induced by high-angle waves. *Nature*, 414, 296-300.
- Battjes, J.A., and J.P.F.M Janssen. 1978. Energy loss and set-up due to breaking of random waves, *Proceedings 16th International Conference on Coastal Engineering*, ASCE, 570-587.
- Caljouw, M., 2000. Video-based monitoring of the Egmond beach- and shoreface nourishment. Evaluation of the 1999 nourishments with the help of the Argus video system. MSc. thesis Delft University of Technology, Department of Hydraulic and Geotechnical Engineering. *Delft Hydraulics Report Z2773*.

- De Vriend, H.J., 1991. Mathematical modelling and large-scale coastal behaviour, Part 1: physical processes. *Journal of Hydraulic Research*, 29, 727-740.
- Falques, A., 2006. Wave driven alongshore stability of the Dutch coastline. *Coastal Engineering*, 53, 243-254.
- Falques, A., and D. Calvete, 2005. Large-scale dynamics of sandy coastlines: diffusivity and instability. *Journal of Geophysical Research*, 110, C03007, doi:10.1029/2004JC002587.
- Nipius, L.J., 2002. Evaluation of nourishment at Egmond with Argus video monitoring and Delft3D-MOR. MSc. thesis Delft University of Technology, Department of Hydraulic and Geotechnical Engineering. *Delft Hydraulics Report Z2822*.
- North, G.R., T.L. Bell, and R.F. Cahalan. 1982. Sampling errors in the estimation of empirical orthogonal functions. *Monthly Weather Review*, 110, 699-706.
- Shand, R.D., D.G. bailey, and M.J. Shepherd. 2001. Longshore realignment of shore-parallel sand bars at Wanganui, New Zealand. *Marine Geology*, 179, 147-161.
- Stive, M.J.F., Aarninkhof, S.G.J, Hamm, L., Hanson, H., Larson, M., Wijnberg, K.M., Nicholls, R.J., Capobianco, M., 2002. Variability of shore and shoreline evolution. *Coastal Engineering*, 47, 211-235.
- Van Duin, M.J.P., N.R. Wiersma, D.J.R. Walstra, L.C. van Rijn, M.J.F. Stive. 2004. Nourishing the shoreface: observations and hindcasting of the Egmond case, The Netherlands. *Coastal Engineering*, 51, 813-837.
- Winant, C.D., Inman, D.L., Nordstrom, C.E., (1975). Description of seasonal beach changes using empirical eigenfunctions. *Journal of Geophysical Research*, 80, 1979-1986.
- Wijnberg, K.M., 2002. Environmental controls on decadal morphologic behaviour of the Holland coast. *Marine Geology*, 189, 227-247.
- Wijnberg, K.M., and F.C.J. Wolf, 1994. Three-dimensional behavior of a multiple bar system. *Proceedings of Coastal Dynamics '94*, ASCE, 59-73.
- Wijnberg, K.M., and A. Kroon. 2002. Barred beaches. *Geomorphology*, 48, 103-120.
- Wijnberg, K.M. and S.G.J. Aarninkhof, 2003, Monthly evolution of a nourished barred beach. *WL|Delft Hydraulics Report Z3290*, 49 pp.

KEYWORDS – ICCE 2006

RESPONSE OF A SHORELINE SANDWAVE TO BEACH NOURISHMENT

K.M. Wijnberg, S.G.J. Aarninkhof, R. Spanhoff

Abstract number: 1683

Beach evolution

Beach nourishment

EOF-analysis

Shoreline change

Shoreline sand wave